

Numerical Simulation on Slabs Dislocation of Zipingpu Concrete Face Dam During Wenchuan Earthquake Based on a Generalized Plasticity Model



Zou Degao

The State Key Laboratory of Coastal and Offshore Engineering, Dalian University of Technology, Dalian, 116024

Xu Bin

The State Key Laboratory of Coastal and Offshore Engineering, Dalian University of Technology, Dalian, 116024

Kong Xianjing

The State Key Laboratory of Coastal and Offshore Engineering, Dalian University of Technology, Dalian, 116024

Zhou Yang

The State Key Laboratory of Coastal and Offshore Engineering, Dalian University of Technology, Dalian, 116024

SUMMARY

The Zipingpu CFRD with the maximum dam height of 156m is the highest embankment dam experiencing the strong shallow earthquake of IX-X degrees in the world. One of the earthquake damages is the slabs dislocation. In this study, a Finite Element procedure was developed to simulate the dynamic response of CFRDs, using the Zipingpu CFRD in China as an illustrative example. The rockfill materials were described through a modified generalized plasticity model, while the interfaces between face slabs and cushions were modelled using zero-thickness interface elements that follow a perfect elasto-plastic model in the tangential direction. The model parameters were calibrated by large-scale triaxial tests and direct shear tests. The results indicated that the finite element procedure based on a modified generalized plasticity model and a perfect elasto-plastic interface model can be used to evaluate the damage of face-slabs of concrete face rockfill dam during earthquake.

Keywords: dislocation; generalized plasticity model; face-slab; concrete face rockfill dam; construction joint; Wenchuan earthquake

1. GENERAL INSTRUCTIONS

A large earthquake ($M_s=8.0$) occurred on May 12, 2008 in Wenchuan, Sichuan Province, China. Besides having a large magnitude, the hypocenter was as shallow as 14 km. The length of the rupture was nearly 240 km and the duration of the main shock was about 80 seconds. Zipingpu CFRD is located 17km west of epicenter and the dam was the highest CRFD (with the height about 150 m) that has ever been subjected to such strong shaking. There were extensive dislocations of face-slabs along construction joints between second and third stages. The phenomenon of dislocation of face-slabs was previously summarized (Chen et al. 2008; Guan 2009). The damage mechanism of Zipingpu CFRD was also analyzed (Chen et al. 2008) based on field investigation. It was concluded that dislocations of face-slabs were due to the permanent deformation of the dam and the lower strength of the construction joints as compared to the concrete slabs. However, most of these summaries are phenomenological in nature. There have been few numerical studies until now.

Dynamic response analysis is an important technique for CFRDs seismic hazards simulation. The equivalent linear analysis based on viscoelastic constitutive models (Hardin 1972) is the main method used currently for the dynamic response analysis of high CFRDs (Uddin and Gazetas. 1995; Succarieh et al. 1993; Samiento et al. 2004). However, the equivalent linear analysis cannot be used to reasonably evaluate the seismic residual deformation of the dam, which is important for the seismic design of high CFRDs. To overcome this disadvantage, two approximate approaches are usually used to evaluate the seismically-induced residual deformation of embankment dams. One is the limit

equilibrium method for rigid block - Newmark sliding block analysis (Newmark 1965) - based on the yield acceleration concept and the other one is the global deformation method based on the strain potential concept (Serff et al. 1976). However, in the above two approaches dynamic response analysis and residual deformation calculation process are not uniform.

In the generalized plasticity theory, the yield surface and plastic potential are not explicitly defined. Instead, direction vectors are used. With appropriate formulations for the direction of plastic flow, loading-unloading directions and plastic moduli, salient behavior of soil can be described. Thus, generalized plasticity allows a less complicated simulation of experimental results for different loading conditions. This theory was introduced and applied to geomaterials (Mroz and Zienkiewicz 1984) and was developed by Zienkiewicz and Pastor (Pastor and Zienkiewicz 1990).

Recently, several improvements including anisotropy, the effects of principle stress rotation and the pressure-level dependency on the generalized plasticity model have been proposed (Pastor et al. 1993; Sassa and Sekiguchi 2001; Ling and Liu 2003; Ling and Yang 2006). Besides, the generalized model was modified to better consider the pressure dependency of rockfill materials under loading, unloading and reloading conditions, and the modified model has been successfully used to simulate the construction process of Zipingpu dam (Xu et al. 2012). In this paper, dynamic numerical simulation based on modified generalized plastic model was carried out to understand the behavior of the mechanism of the slab dislocation during the Wenchuan earthquake.

3. DAMAGE OF ZIPINGPU DAM DURING WENCHUAN EARTHQUAKE

Zipingpu CFRD was obviously damaged during Wenchuan earthquake (Chen et al. 2008; Guan 2009). There are apparent settlements on the crest of the dam as shown in Figure 1 (a). The field observed maximum settlement at dam crest reach at 0.9-1.0 m, including a separation void of 0.15 - 0.20 m in height (Guan 2009). Serious dislocation damage also occurred between the stage II and III slabs at EL. 850 m, as shown in Figure 1 (b).



(a) Crest settlement



(b) Dislocations of the construction joints

Figure 1. Crest settlement and dislocations of face-slabs along construction joints

4. CONSTITUTIVE MODEL

4.1. Generalized plasticity model for rockfills

In this study, the modified generalized model was used for rockfill materials. Detailed describe of the constitutive models for rockfills are referred as Xu et al. (Xu et al. 2012)

4.2. Interface Element and Model Behavior

Goodman contact elements (Goodman et al. 1968) with zero thickness, as shown in Figure 2, were applied to model the interface between face slabs and rockfills. Same elements were also applied for simulating slabs joints and peripheral joints. The relationship between force and displacement of contact element is expressed as:

$$\begin{Bmatrix} \Delta\tau_{xy} \\ \Delta\sigma_y \end{Bmatrix} = \begin{Bmatrix} k_{xy} & 0 \\ 0 & k_{yy} \end{Bmatrix} \begin{Bmatrix} \Delta\delta_{xy} \\ \Delta\delta_{yy} \end{Bmatrix} \quad (4.1)$$

where $\Delta\tau_{xy}$ is the incremental shear stresses, k_{xy} is the shear stiffness, and $\Delta\delta_{xy}$ is the incremental shear displacements in the shear direction. $\Delta\sigma_y$ is incremental normal stress, k_{yy} is the normal stiffness and $\Delta\delta_{yy}$ is the incremental normal displacement.

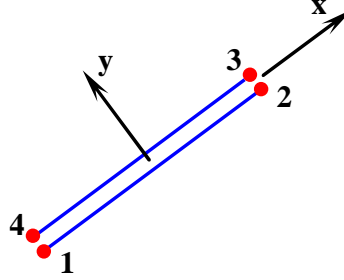


Figure 2. Sketch diagram of a Goodman element

The perfect elasto-plastic interface model depending pressure level was used for interface between face slabs and rockfills. The stiffness in the tangent and normal directions of the contact element can be expressed as:

$$k_{xy} = k_1 p_a \left(\frac{\sigma_y}{p_a} \right)^n \quad \tau_{xy} < c + \sigma_y \operatorname{tg} \varphi \quad (4.2)$$

$$k_{xy} = 0 \quad \tau_{xy} > c + \sigma_y \operatorname{tg} \varphi$$

$$k_{yy} = k_2 \quad \text{under compression} \quad (4.3)$$

$$k_{yy} = 0 \quad \text{under tension} \quad (4.4)$$

where p_a is the atmospheric pressure; k_{xy} is the tangential coefficients of shear stiffness; k_1 is the modulus factor; n is the modulus exponent; φ is the internal friction angle of the contact surface; σ_y is the normal stress; τ_{yx} is the shear stresses, and c is the interface cohesion; k_2 is the compressive stiffness.

The linear elastic interface mode was used for slab joints and peripheral joints. The stiffness in the normal direction is expressed in Equations (4.3) and (4.4). The stiffness in the tangential directions of the contact element can be expressed as:

$$k_{xy} = k_1 \quad (4.5)$$

5. PARAMETERS OF MATERIALS

5.1. Slabs

Linear elastic model was used to simulate the concrete face slabs. According to the design information of the concrete face slabs, the detailed parameters were taken as density $\rho = 2.40 \text{ g/cm}^3$, elastic modulus $E = 28000 \text{ MPa}$ and Passion's ratio $\nu = 0.167$.

5.2. Rockfill Materials

The parameters of rockfills are given in Table 1 (Xu et al. 2012).

Table 5.1. Parameters of rockfills

G_0	K_0	M_g	M_f	α_f	α_g	H_0	H_{U0}	m_s
1000	1400	1.8	1.38	0.45	0.4	1800	3000	0.5
m_v	m_1	m_u	r_d	γ_{DM}	γ_u	β_0	β_1	
0.5	0.2	0.2	180	50	4	35	0.022	

5.3. Interface

The interface between the concrete slab and the cushion of the Zipingpu CFRD was experimentally studied (Zhang and Zhang 2008). Based on the tests results, the parameters of the perfect elasto-plastic interface model were determined and listed in Table 2.

Table 5.2. Parameters of interface

k_1	k_2	n	$\varphi / ^\circ$	c / MPa
300	1e10	0.8	41.5	0

5.4. Construction Joints

Shear strength is one of the basic mechanical properties of concrete material. Hofbeck (Hofbeck et al. 1969) obtained the ratio 0.119~0.316 of concrete shear strength to compressive strength through extensive testing. The shear strength of concrete was deduced (Li et al. 1993) and expressed as

$$\tau_0 = \frac{1}{2} \cdot \sqrt{f_c \cdot f_t} \quad (5.1)$$

where f_c is the axial compressive strength of concrete and f_t is the axial tensile strength of concrete. This formula was used in the present study to calculate the shear strength of the face-slab concrete and a value of 2.73 MPa was obtained according to the concrete grade.

The strength of the concrete at the construction joints is only about 50% of integral cast (Jensen 1975). When seismic force acts on the joint, the strength of the concrete would decrease up to 30%. Therefore, the dynamic shear strength of the construction joints was assumed to be 0.545 MPa in this study. In this study, the shear stiffness k_1 of the construction joints is taken as 0.12 MPa/m according to Equation (4.2). The compressive stiffness is taken as 25000 MPa/m. Parameters of the construction joints are given in Table 5.3.

Table 5.3. Parameters of construction joints

k_1	k_2	n	φ	c / MPa
1.2e5	2.5e10	0	0	0.545

6. FE ANALYSIS

6.1. FE Mesh

The 2-D FE mesh of Zipingpu dam is shown in Figure 3. The rockfill materials and slabs are simulated by Quadratic elements. The difference of the horizontal displacement of node 166 and node 165 was defined as dislocation value. The bottom boundary of the dam is fixed at both x and y direction.

6.2. Input ground motions

As no bedrock acceleration time histories were recorded at the dam site during Wenchuan earthquake, bedrock acceleration time histories measured at Mao Town, which is located 75 km from Zipingpu Dam, was adopted as input ground motions scaled to have a PGA of 0.55g (Kong et al. 2010), and the vertical one was assumed to be 2/3 of the horizontal. The acceleration time histories are shown in Figure 4.

6.3. Damping

Similar to other hysteresis models for soils, the generalized plasticity model can capture the material damping at finite strain but predicts much smaller damping than that of actual soils at infinitesimal strain. Rayleigh damping was used to compensate for this deficiency. A viscous damping ratio of 5% was assumed for the rockfill materials. The same damping ratio was also assumed for the concrete slabs.

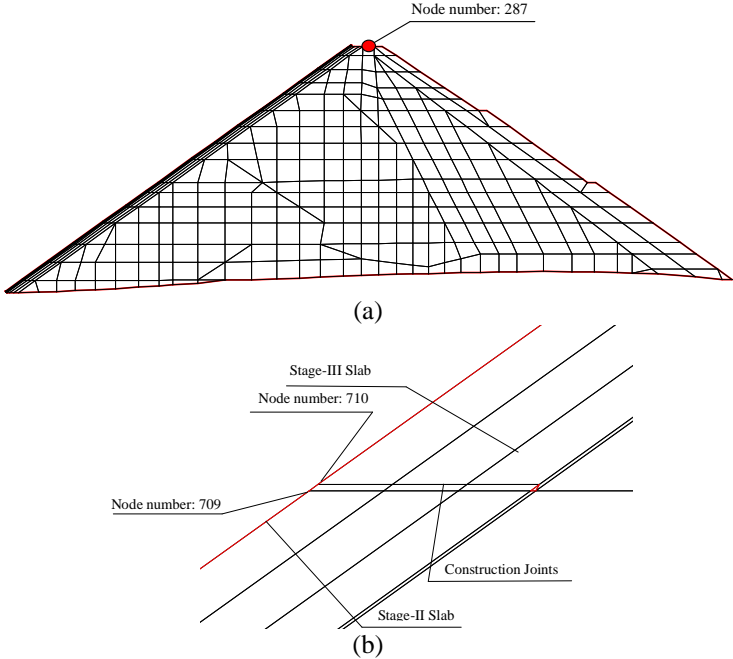
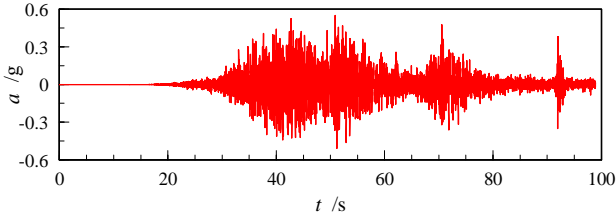
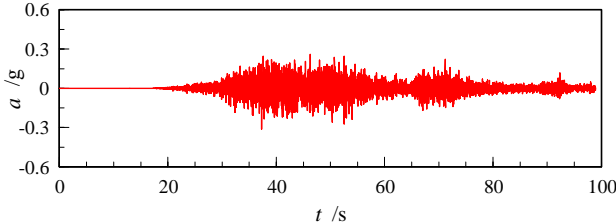


Figure 3. 2-D FE mesh of Zipingpu CFRD



(a) Horizontal direction



(b) Vertical direction

Figure 4. Acceleration time histories

7. RESULTS AND ANALYSIS

Firstly, static analysis was carried out to simulate the process of dam construction and water storage. Secondly, dynamic response analysis was performed, in which the dynamic water pressure was simulated by adding mass method (Westergaard 1933).

7.1. Settlement

The crest settlement history during earthquake is illustrated as Figure 5. Figure 6 shows the contours of settlement at the end of earthquake. The maximum crest settlement is 0.98 m, and the settlement at EL. 850 is 0.84 m, which agrees well with the field measured results (Chen et al. 2008).

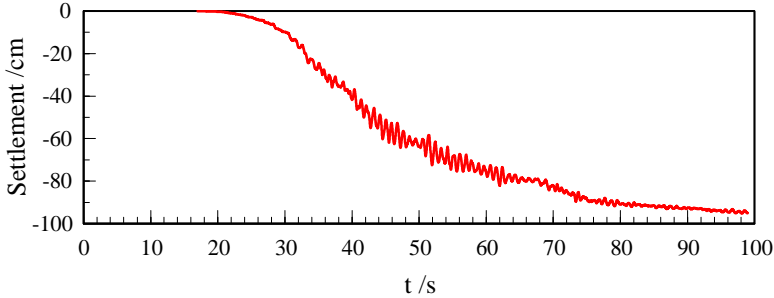


Figure 5. Crest settlement history of Zipingpu dam during Wenchuan earthquake

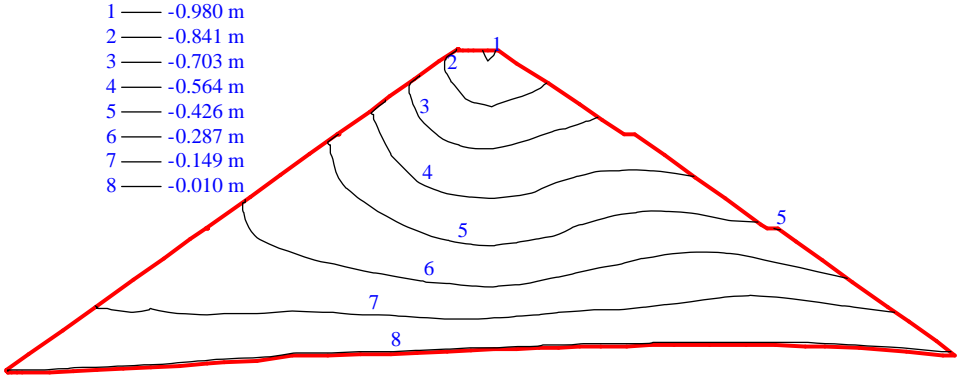
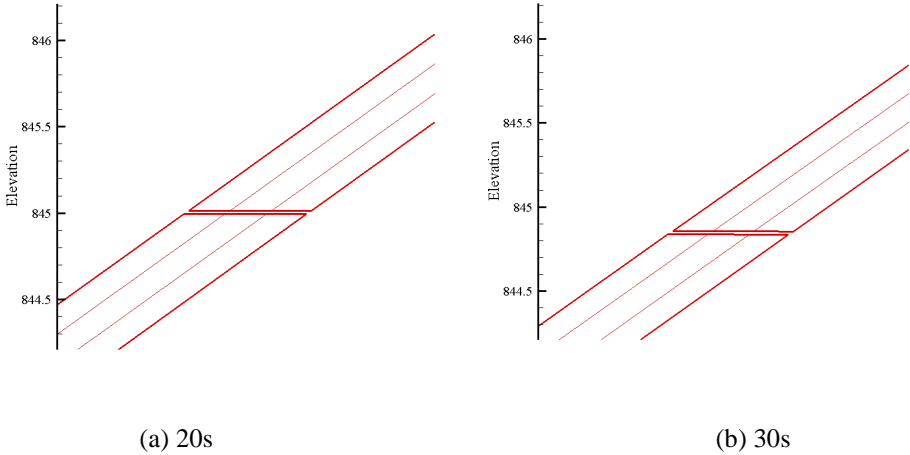
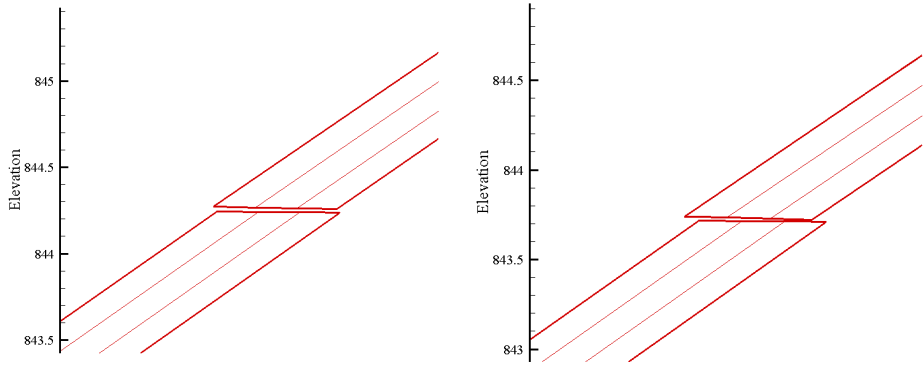


Figure 6. Settlement of Zipingpu dam

7.2. Slabs Dislocation

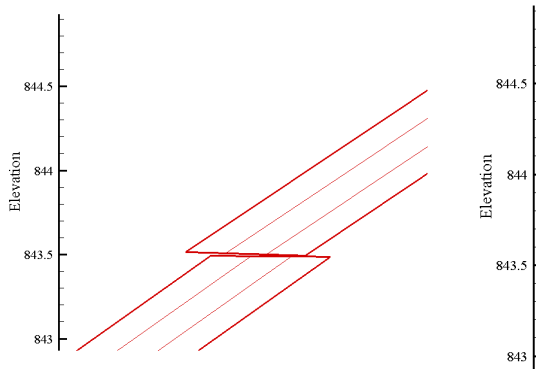
The slabs dislocation development diagram and history are shown in Figure 7 and Figure 8 during Wenchuan earthquake, respectively. It can be seen from the figure that the slabs dislocation was development gradually during the shaking. The cumulative dislocation reached as 9.1 cm at the end of earthquake. It was reported by the in situ investigations (Chen et al. 2008) that the dislocations were 2-17cm after Wenchuan earthquake. The results in this study agree well with the measured results. The dislocation phenomenon was successfully simulated in the view of qualitative point by the modified generalized plasticity model.





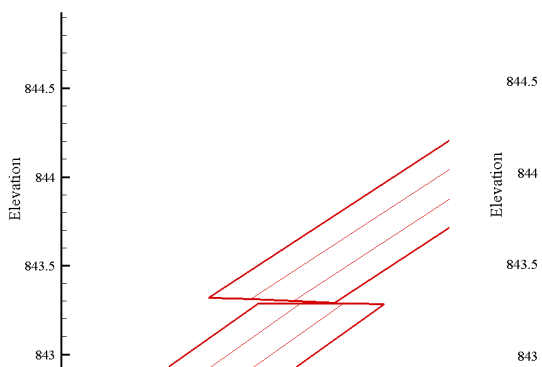
(c) 40s

(d) 50s



(e) 60s

(f) 70s



(g) 80s

(h) 90s

Figure 7. The slabs dislocation of different time during earthquake

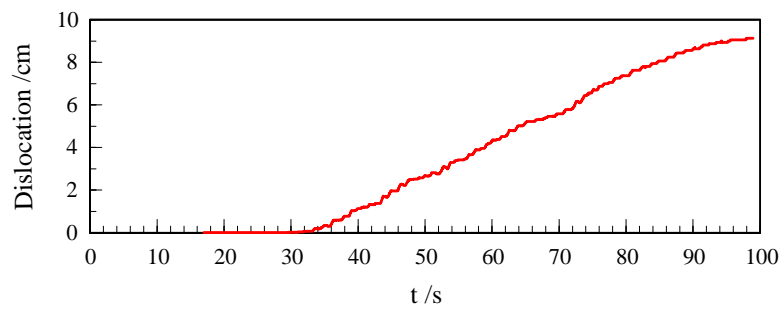


FIGURE 8. THE SLABS DISLOCATION DURING EARTHQUAKE.8. CONCLUSIONS

The modified generalized plasticity model could be used to calculate directly the residual deformation of dam during earthquake. The slabs dislocation occurred at the construction joints of face-slab between the second and third stage under strong shaking, was successfully simulated in this study. The finite element procedure based on a modified generalized plasticity model and a perfect elasto-plastic interface model can be used to evaluate the damage of face-slabs of concrete face rockfill dam during earthquake.

ACKNOWLEDGEMENTS

This research was supported by the National Natural Science Foundation of China (No. 51138001, 51078061, 50908032) and the Fundamental Research Funds for the Central Universities of China (No. DUT11ZD110, DUT12LK37). The supports are gratefully acknowledged.

APPENDIX A:

Generalized plasticity model for sand (Pastor, 1990)

In plasticity theory, the strain increment can be decomposed into two parts

$$d\boldsymbol{\varepsilon} = d\boldsymbol{\varepsilon}^e + d\boldsymbol{\varepsilon}^p \quad (\text{A.1})$$

where $d\boldsymbol{\varepsilon}^e$ is incremental elastic strain tensor, and $d\boldsymbol{\varepsilon}^p$ is incremental plastic strain tensor.

The stress-strain relationship is expressed as:

$$d\boldsymbol{\sigma}' = \mathbf{D}^{ep} : d\boldsymbol{\varepsilon} \quad (\text{A.2})$$

In generalized plasticity theory, the elasto-plastic stiffness tensor is expressed as:

$$\mathbf{D}^{ep} = \mathbf{D}^e - \frac{\mathbf{D}^e : \mathbf{n}_g : \mathbf{n}^T : \mathbf{D}^e}{H + \mathbf{n}^T : \mathbf{D}^e : \mathbf{n}_g} \quad (\text{A.3})$$

where

$d\boldsymbol{\sigma}'$: incremental effective stress tensor

$d\boldsymbol{\varepsilon}$: incremental strain tensor

\mathbf{D}^{ep} : elasto-plastic stiffness tensor

\mathbf{D}^e : elastic stiffness tensor

\mathbf{n} : loading direction vector

\mathbf{n}_g : flow direction vector

H : plastic modulus

The distinction between loading and unloading directions is described through the following criteria:

$$\mathbf{n} : d\boldsymbol{\sigma}^e > 0 \quad (\text{loading}) \quad (\text{A.4a})$$

$$\mathbf{n} : d\boldsymbol{\sigma}^e < 0 \quad (\text{unloading}) \quad (\text{A.4b})$$

where $d\boldsymbol{\sigma}^e$ is the elastic stress increment.

The following generalized expression is proposed for the stress-dilatancy relationship (Nova, 1982):

$$d_g = \frac{d\varepsilon_v^p}{d\varepsilon_s^p} = (1 + \alpha_g)(M_g - \eta) \quad (\text{A.5})$$

where $d\varepsilon_v^p$ and $d\varepsilon_s^p$ are the incremental plastic volumetric and deviatoric strains, respectively. M_g is the slope of the critical state line in the $p' - q$ plane, $\eta = q/p'$ is the stress ratio, and α_g is a model parameter.

M_g is related to the angle of internal friction at the critical state ϕ_g' and Lode's angle θ following the smoothed Mohr-Coulomb criterion proposed by Zienkiewicz and Pande (Zienkiewicz, 1977):

$$M_g = \frac{6 \sin \phi'_g}{3 - \sin \phi'_g \sin 3\theta} \quad (\text{A.6})$$

The flow direction vector in triaxial space is then defined as:

$$\mathbf{n}_g^T = (n_{gv}, n_{gs})$$

with $n_{gv} = d_g / \sqrt{(1+d_g^2)}$ and $n_{gs} = 1 / \sqrt{(1+d_g^2)}$.

Non-associated flow rule is assumed in the model and the loading direction vector is defined as:

$$\mathbf{n}^T = (n_v, n_s)$$

with $n_v = d_f / \sqrt{(1+d_f^2)}$, $n_s = 1 / \sqrt{(1+d_f^2)}$ and $d_f = (1 + \alpha_f)(M_f - \eta)$. Here M_f and α_f are both model parameters.

The elastic behavior is defined by the shear and bulk moduli:

$$K = K_0 \frac{p'}{p'_0} \quad (\text{A.7})$$

$$G = G_0 \frac{p'}{p'_0} \quad (\text{A.8})$$

Where K_0 , G_0 are the elastic volumetric and shear moduli respectively, p' is the mean effective stress, and p'_0 is a reference value.

The plastic modulus under loading and reloading is defined as:

$$H_L = H_0 \cdot p' \cdot H_f \cdot (H_v + H_s) \cdot H_{DM} \quad (\text{A.9})$$

$$H_f = (1 - \eta / \eta_f)^4 \quad (\text{A.10})$$

$$\eta_f = (1 + 1/\alpha_f) M_f \quad (\text{A.11})$$

$$H_v = 1 - \eta / M_g \quad (\text{A.12})$$

$$H_s = \beta_0 \beta_1 \exp(-\beta_0 \xi) \quad (\text{A.13})$$

$$H_{DM} = \left(\frac{\zeta_{\max}}{\zeta} \right)^{\gamma_{DM}} \quad (\text{A.14})$$

$$\zeta = p' \cdot \left[1 - \left(\frac{1 + \alpha_f}{\alpha_f} \right) \cdot \frac{\eta}{M_f} \right]^{1/\alpha_f} \quad (\text{A.15})$$

where H_0 is the plastic modulus number; H_f , H_v , and H_s are plastic coefficients; $\xi = \int |d\epsilon_s^q|$ is the accumulative plastic strain; and β_0 , β_1 , and γ_{DM} are model parameters.

The plastic modulus under unloading is defined as:

$$H_u = H_{u0} \left(\eta_u / M_g \right)^{-\gamma_u} \quad \left| \eta_u / M_g \right| < 1 \quad (\text{A.16})$$

$$H_u = H_{u0} \quad \left| \eta_u / M_g \right| \geq 1 \quad (\text{A.17})$$

Generalized plasticity model modified for rockfills (Xu et al. 2012)

The original model was mainly used for sand liquefaction analysis with small effective confining pressure. However, the confining pressure varies from 0 to 3 MPa for high rockfill dams. In this paper, to better consider the wide range of the confining pressure and the associated particle crushing on the response of rockfills in the dam, which differs from that of sandy liquefaction problem, Equations

(A.7-9 and A.16) were modified as:

$$K = K_0 p_a (p' / p_a)^{m_v} \quad (\text{A.18})$$

$$G = G_0 p_a (p' / p_a)^{m_s} \quad (\text{A.19})$$

$$H_L = H_0 \cdot p_a \cdot (p' / p_a)^{m_l} \cdot H_f \cdot (H_v + H_s) \cdot H_{DM} \cdot H_{den} \quad (\text{A.20})$$

$$H_u = H_{u0} \cdot p_a \cdot (p' / p_a)^{m_u} \cdot (\eta_u / M_g)^{-\gamma_u} \cdot H_{den} \quad \left| \eta_u / M_g \right| < 1 \quad (\text{A.20})$$

Where p_a is the atmospheric pressure (equals to 100 kPa); H_{DM} is also modified as $e^{(1-\eta/\eta_{\max})\gamma_{DM}}$ in this study; η_{\max} is the largest value of the stress ratio ever reached; $H_{den} = \exp(-\gamma_d \epsilon_v)$ is the densification coefficient, which takes into account the effects of cyclic hardening as proposed in Ling and Liu (Ling and Liu, 2003).

All of the exponents for K , G , H_L , and H_u were defined as 0.5 for sandy soils in Ling and Liu (Ling and Liu, 2003), which may not be appropriate for rockfills. In particular, rockfill materials exhibit considerable particle crushing under modest confining pressure and shear stress while most sandy soil particles are much less crushable.

REFERENCES

- Chen S. S., Huo J.P., Zhang W.M.. (2008). Analysis of effects of “5.12” Wenchuan Earthquake on Zipingpu Concrete Face Rock-fill Dam. *Chinese Journal of Geotechnical Engineering*, **30:6**, 795-801. (in chinese)
- Guan Z. C. (2009). Investigation of the 5.12 Wenchuan Earthquake damages to the Zipingpu Water Control Project and an assessment of its safety state. *Science China Series E-Tech Science*, **52:4**, 820-834.
- Hardin B. O., Drnevich V. (1972). Shear modulus and damping in soils. *Journal of Soil Mechanics and Foundation Division* **98:7**, 667-692.
- Uddin N., Gazetas G. (1995). Dynamic response of concrete-faced rockfill dams to strong seismic excitation. *Journal of Geotechnical Engineering*, **121:2**, 185-197.
- Succarieh M, Elgamal A-W, Yan L. (1993). Observed and predicted earthquake response of La Villita Dam. *Journal of Engineering Geology*, **34:3**, 11-26.
- Samiento N, Romo M, Marinez S, Marengo H. (2004). Seismic behavior of concrete- faced rockfill dams, considering a spatial variation of variation of motion along the rigid base. *In: Proceedings of the 13th world conference on earthquake engineering*. Paper No. 85.
- Newmark. N. M. (1965). Effects of earthquakes on dams and embankments. *Geotechnique* **15:2**, 139-160.
- Serff, N., Seed, H. B., Makdisi, F. I., and Chang, C. K. (1976). Earthquake Induced Deformations of Earth Dams. *Report No. EERC/76 -4, Earthquake Engineering Research Center*, University of California, Berkeley
- Mroz Z., Zienkiewicz O. C. (1984). Uniform formulation of constitutive equations for clay and sand. *Mechanics of engineering materials*, C. S. Desai, R. H. Gallanher. New York, Wiley, 415-450.
- Pastor M., Zienkiewicz O. C. (1990). Generalized plasticity and the modeling of soil behavior. *Int. J. Numer. Analyt. Meth. Geomech.*, **14:3**, 151-190.
- Pastor M., Zienkiewicz O. C., Xu G. D. et al. (1993). Modeling of sand behavior: Cyclic loading, anisotropy and localization. *Modern approaches to plasticity*, D. Kolymbas. New York, Elsevier, 469-492.
- Sassa S., Sekiguchi H. (2001). Analysis of waved-induced liquefaction of sand beds. *Geotechnique*, **51:2**, 115-126.
- Ling H. I., Liu H. (2003). Pressure dependancy and densification behavior of sand through a generalized plasticity model. *Journal of Engineering Mechanics, ASCE*, **129:8**, 851-860.
- Ling H. I., Yang S. (2006). Unified sand model based on the critical state and generalized plasticity. *Journal of Engineering Mechanics, ASCE*, **132:12**, 1380-1391.
- Xu B, Zou Degao, Liu Huabei. (2012). Three-dimensional simulation of the construction process of the Zipingpu concrete face rockfill dam based on a generalized plasticity model. *Comput Geotech*, **43:6**, 143-154.
- Westergaard H. M. (1933). Water pressures on dams during earthquakes. *Trans. ASCE*, **98**: 418-433.
- Hofbeck J. A., Ibrahim I. O., Mattock A. H. (1969). Shear Transfer in Reinforced Concrete. *ACI Journal*, **2**: 119-128.
- Li Hong, Liu Xila. (1993). The Critical Tensile-shear Failure and Shear Strength of Concrete. *Engineering Mechanics*, **10:1**, 52-60.
- Jensen B. C. (1975). Lines of discontinuity for displacements in the theory of plasticity of plain and reinforced concrete. *Magazine of Concrete Research*, **27:92**, 143-150.
- Kong Xianjing, Zhou Yang, Xu Bin et al. (2010). Analysis on Seismic Failure Mechanism of Zipingpu Dam and Several Reflections of Aseismic Design for High Rock-fill Dam. *Engineering, Science, Construction, and Operations in Challenging Environments, Hawaii*

- Pastor M., Zienkiewicz O. C. (1990). Generalized plasticity and the modeling of soil behavior. *Int. J. Numer. Analyt. Meth. Geomech.*, **14:3**, 151-190.
- Nova, R. (1982). A constitutive model under monotonic and cyclic loading. *In Soil mechanics-transient and cyclic loads*. Edited by G. Pande and O.C. Zienkiewicz. John Wiley & Sons, Ltd., New York, 343-373.
- Zienkiewicz O. C., and Pande, G. N. (1977). Some useful forms of isotropic yield surface for soil and rock mechanics. *Finite Elements in Geomechanics*, G. Gudehus, eds., Wiley, New York, 179-190.
- Ling H. I., Liu H. (2003). Pressure dependancy and densification behavior of sand through a generalized plasticity model. *Journal of Engineering Mechanics*, ASCE, **129:8**, 851-860.